

Lithium battery charge state estimation based on improved Unscented Kalman filtering

Changchang Li^{1*}

¹ School of Shipping, Shandong Jiaotong University, Weihai 264200, China

*Corresponding author Email: 1430564954@qq.com

Received 8 May 2025; Accepted 12 June 2025; Published 1 September 2025

© 2025 The Author(s). This is an open access article under the CC BY license.

Abstract: The state of charge (SOC) of lithium batteries is one of the key parameters to ensure their safe operation. In response to the traditional untraceable Kalman filtering (UKF) algorithm in the process of estimating the state of charge (SOC), the covariance matrix is non-positively determined, which leads to the termination of the algorithm. In this paper, an improved trace-free Kalman filtering method with singular value decomposition Unscented Kalman filtering (SVD-UKF) is proposed to estimate the SOC. singular value decomposition is used instead of Cholesky decomposition to improve the accuracy and stability of SOC estimation. First, a second-order RC equivalent circuit model is established, a lithium battery experimental platform is built to obtain charge/discharge data, and the parameters of the second-order RC model are identified by combining the hybrid pulse charge/discharge test and the 1stopt software, and then the battery SOC estimation is carried out by using the improved untraceable Kalman filtering algorithm, and the SVD-UKF estimation results have a smaller error with the actual value compared with the traditional UKF through experimental analysis, the estimation accuracy is high, and the real value can be converged quickly when the initial value is inaccurate, and the average absolute error is reduced by about 14.5% compared with the traditional UKF, which has good accuracy and robustness.

Keywords: lithium battery, state of charge, equivalent circuit model, Unscented Kalman filtering algorithm.

1. Introduction

Lithium-ion batteries are widely used in electric vehicles, portable electronic devices and energy storage systems due to their high energy density, long life and environmental friendliness. However, in order to ensure the safety and longevity of batteries, it is crucial to accurately estimate their state-of-charge (SOC), which reflects the amount of charge remaining in the battery and is one of the core parameters in a battery management system (BMS)^[1]. Accurate SOC estimation not only prevents overcharging or overdischarging, but also improves energy utilization and extends battery life^[2].

Currently, common SOC estimation methods include the ampere-time integration method, open-circuit voltage method, data-driven method, and Kalman filter method. However, the complex electrochemical characteristics of lithium batteries make these methods have certain limitations in practical applications. The ampere-time integration method is used to estimate the SOC by integrating the battery current over time, which has the advantage of being simple to implement and convenient to calculate, but its accuracy depends on the precision of the initial SOC value, and it is susceptible to the effect of the accumulated error of the current noise in long-time operation. The open-circuit voltage method establishes the relationship between open-circuit voltage and SOC by utilizing the open-circuit voltage test data of the battery in the offline state^[3]. This method can only achieve accurate estimation when the battery is in a long-term resting state. The data-driven method estimates the SOC by fitting a functional relationship between the battery terminal voltage value, current value, temperature value, other input parameters, and the SOC value. however, the data-driven method requires higher data quality and larger data

volume. Therefore, there are still great difficulties in practical applications^[4].

The Kalman filter (KF) algorithm has become one of the popular methods for SOC estimation in recent years due to its ability to adapt to a wide SOC range and effectively reduce the effects of measurement errors and sensor noise^[5]. KF solves the estimation problem of a system by equating the state equations in the circuit. However, when the system presents nonlinearity, LKF cannot provide satisfactory estimation results. The UKF algorithm updates the corrected a posteriori estimate and covariance by selecting a set of sampling points that satisfy specific requirements. Especially in the strong nonlinear filtering system, the filtering effect of UKF is more significant compared to EKF^[6]. It is worth noting that when using the UKF algorithm, the error covariance matrix must be a positive definite matrix; a non-positive definite error covariance matrix will cause the system to diverge, resulting in the UKF algorithm not being able to proceed.

In order to further improve the estimation accuracy and stability, this paper proposes an improved trace-free Kalman filtering method using the UKF algorithm as the basis and the singular value decomposition instead of the Cholesky decomposition to estimate the SOC of the battery, and analyzes the performance of the method under real working conditions through experiments and simulations to evaluate its potential application in battery management systems.

2. Lithium battery equivalent model and parameter identification

2.1 Lithium battery equivalent model design

The battery model can effectively simulate the operating characteristics of lithium-ion batteries during the charging and discharging process, which is crucial for the analysis, management and control of the battery state. An accurate battery model can not only better reflect the electrochemical process inside the battery, but also provide a solid foundation for the accurate estimation of the battery state of charge (SOC)^[7]. In this paper, the Thevenin equivalent model and the RC parallel network are chosen to characterize the polarization response of the battery, which can effectively describe the dynamic characteristics of the battery during charging and discharging, especially its nonlinear features.

In order to better simulate the polarization process and the dynamic response behavior of the battery, especially in the transition stage of battery charging and discharging, a model that can accurately reflect the polarization process is needed. Therefore, in this paper, the second-order RC equivalent model is selected on the basis of balancing model accuracy and computational resources. By introducing two RC parallel networks, the second-order RC model is able to more accurately describe the complex dynamic response behavior of lithium-ion batteries during the polarization process, especially the performance of the characteristics under multiple time constants^[8]. Compared with the first-order RC model, the second-order model is able to capture more information about the battery dynamics, thus better reflecting the battery characteristics under fast charging and discharging conditions and improving the overall accuracy of the model. As shown in Fig. 1, the open-circuit voltage of the battery is denoted as U_{OC} , the resistor R_0 represents the internal resistance of the battery, U_0 is the voltage across the ohmic internal resistance, I is the load current of the battery, and V_b while is the terminal voltage of the battery. The two RC networks in the model consist of resistor R_1R_2 , and capacitor C_1C_2 , respectively, which are used to characterize the polarization process and dynamic properties of the battery at different time constants. The corresponding voltage sums represent the dynamic responses of the two RC networks. With these two RC parallel networks, the second-order RC model is able to capture the complex electrochemical processes inside the battery while maintaining a low computational complexity^[9].

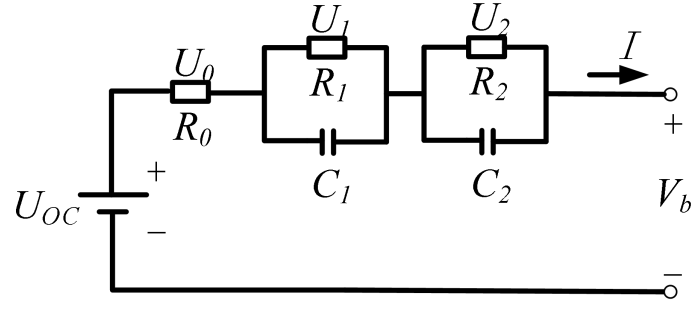


Fig. 1 Second order RC equivalent circuit model of lithium battery

Can be obtained from Kirchhoff's law:

$$V_b = U_{oc} - U_1 - U_2 - IR_0 \quad (1)$$

$$C_1 \frac{dU_1}{dt} = I - \frac{U_1}{R_1} \quad (2)$$

$$C_2 \frac{dU_2}{dt} = I - \frac{U_2}{R_2} \quad (3)$$

The SOC of a lithium battery is defined as the ratio of its residual capacity to its rated capacity, and is calculated by the following formula:

$$SOC(t) = SOC(t_0) - \int_{t_0}^t \frac{\eta I}{Q_n} dt \quad (4)$$

Where: t -time; $SOC(t)$ - t moment lithium battery SOC value; $SOC(t_0)$ - t_0 moment lithium battery SOC value; η -Coulomb efficiency, $\eta=1$; Q_n -rated capacity of lithium battery.

2.2 Parameter Identification

2.2.1 Battery SOC-OCV relationship curve

Before the estimation of the SOC of lithium battery, it is necessary to identify the parameters of its equivalent circuit model, and the object is the saturation voltage of 4.2V, cut-off voltage of 2.5V, the capacity of 2000mA-h lithium ternary battery as a study. The experimental platform is shown in Fig. 2.

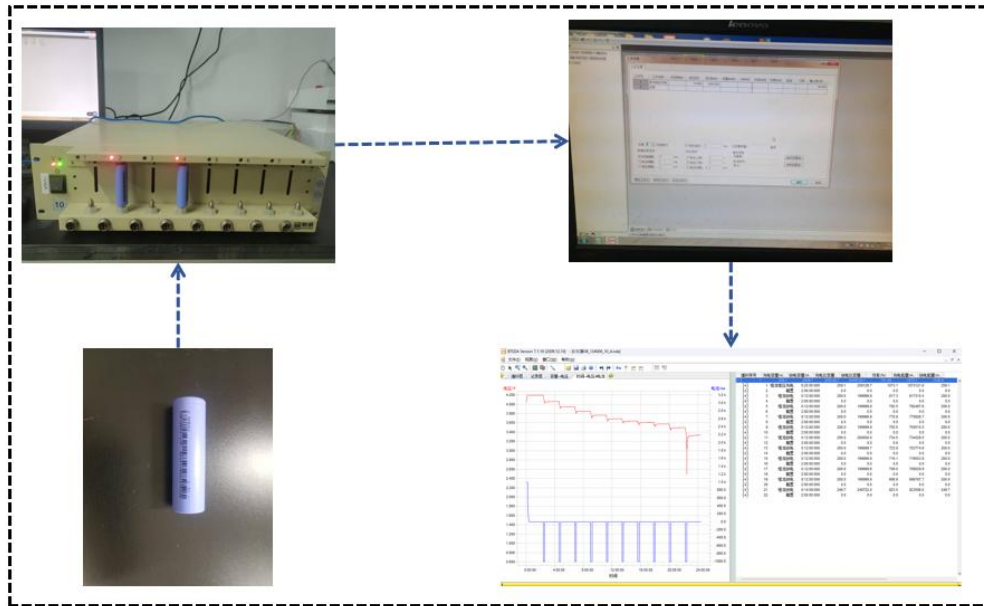


Fig. 2 Battery test platform

Firstly, the mixed pulse power characterization (HPPC) experiments were conducted at a constant temperature of 25 °C with reference to the “FreedomCar Power-Assisted Battery Test Manual”, and the purpose of the

experiments was to determine the relationship between the UOC and SOC of Li-ion batteries and to identify the parameters of Li-ion battery models.

Experimental steps: constant current and constant voltage charging to the cut-off current, stationary for 2h, discharge at a constant current of 0.5C (1000mA) for 12min, stationary for 2h, cyclic discharge until the end of the cut-off voltage, and record the changes in voltage and current. As shown in Figure 3.

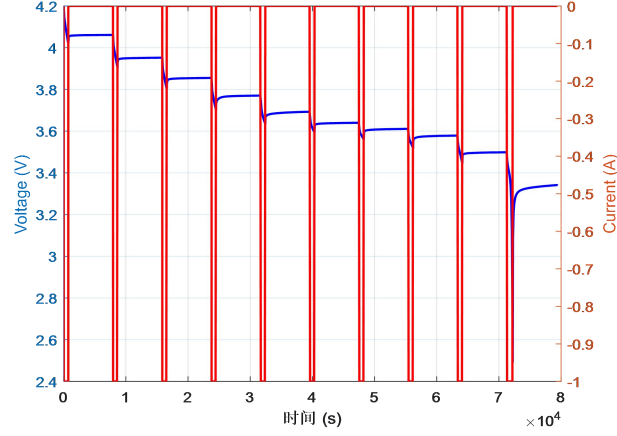


Fig. 3 HPPC current and voltage curves

The relationship equation of SOC-OCV was obtained by HPPC experiment and the curve is shown in Fig. 4.

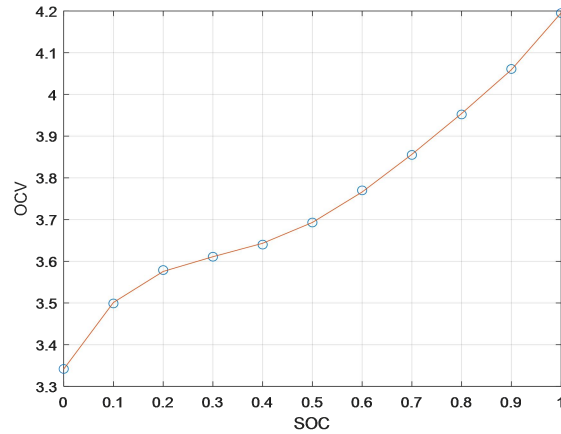


Fig. 4 SOC-OCV relationship plot

A 6th order polynomial was fitted to the SOC-UOC curve to characterize the functional relationship between UOC and SOC:

$$\begin{aligned} OCV(SOC) = & 5.801 * SOC^6 - 12.43 * SOC^5 + 4.254 * SOC^4 + 7.781 * SOC^3 \\ & - 6.739 * SOC^2 + 2.191 * SOC + 3.341 \end{aligned} \quad (5)$$

2.2.2 Parameter Identification by Joint 1stopt Software

Parameter identification can be divided into offline identification and online identification, in which offline identification can make full use of the precise data under experimental conditions, thus ensuring the accuracy of the identification results. In this paper, the method of exponential fitting combined with 1-Stopt software is adopted to carry out offline parameter identification of lithium batteries. Using the HPPC data measured under laboratory conditions as the basis, the internal parameters of the battery are recognized by fitting. As shown in Fig. 5, a certain voltage curve in the HPPC experiment is illustrated as an example.

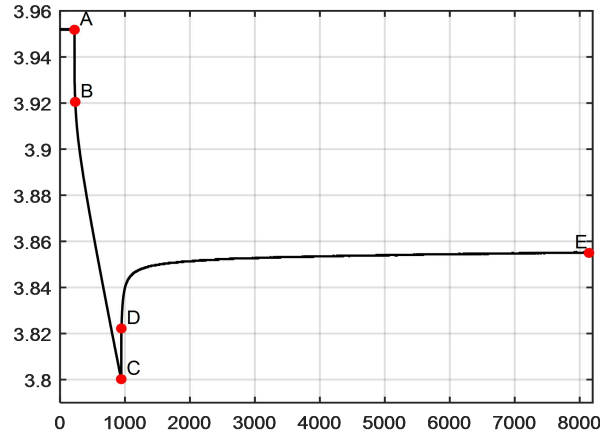


Fig. 5 End voltage response curve

Ohmic internal resistance R_0 identification:

At the beginning and end of the discharge, the battery has not yet polarized. The abrupt changes between points A to B and C to D are due to the ohmic internal resistance. Therefore, R_0 can be expressed as:

$$R_0 = \frac{(U_A - U_B) + (U_D - U_C)}{2I} \quad (6)$$

The voltage of the battery will rise slowly until stabilized in a period of time when the battery is stationary after pulse discharge, and the voltage response of the RC circuit at this moment is the zero-input response. The slow rise of the terminal voltage in the DE section indicates the polarization response process of R_1C_1 and R_2C_2 . The equation for the terminal voltage is:

$$V_b = U_{OC} - U_1 e^{(-t/\tau_1)} - U_2 e^{(-t/\tau_2)} \quad (7)$$

In the above equation, the initial voltages of the two RC links U_1 and U_2 , and represent the time constants of each RC parallel circuit. The time constant is expressed as:

$$\begin{cases} \tau_1 = R_1 \cdot C_1 \\ \tau_2 = R_2 \cdot C_2 \end{cases} \quad (8)$$

The custom fit function can be expressed as:

$$y = a - b * \exp(-ct) - d * \exp(-ft) \quad (9)$$

Based on the experimental data obtained from the Hybrid Pulsed Power Characterization (HPPC) test experiments, the terminal voltage data for the segment of SOC from 100% to 90% were first selected and these experimental data were imported in MATLAB. Next, variables with time as the horizontal coordinate and end voltage as the vertical coordinate were created and the data were simplified as necessary for fitting analysis. Subsequently, the CurveFitting toolbox of MATLAB was utilized to select a custom fitting function for fitting analysis, which was in the form of an exponential function. In order to further improve the fitting accuracy, the other four unknown parameters in the model can be optimized with the help of 1stOpt software to determine the initial values, and the obtained optimized parameters are then returned to MATLAB for initialization and final determination of the parameter values. The same steps can be used for other SOC intervals, and the corresponding resistance, capacitance and other parameters are solved sequentially to construct a complete battery equivalent circuit model. The parameters are identified using 1stopt software and the fitted relational equation in MATLAB, and the results of parameter identification are shown in Table 1.

Table 1 Parameter identification results

SOC	R_0/Ω	R_1/Ω	C_1/F	R_2/Ω	C_2/F
0.1	0.086	0.01714	391	0.008	293289

0.2	0.2525	0.01133	189605	0.0198	6022
0.3	0.0249	0.01588	2872	0.009091	146723
0.4	0.02395	0.00716	277112	0.01398	3288
0.5	0.0231	0.01676	133391	0.01419	7620
0.6	0.0237	0.01562	82874	0.02394	7229
0.7	0.0235	0.02379	2446	0.007319	244157
0.8	0.02305	0.01806	2035	0.00624	327923
0.9	0.0226	0.01379	1994	0.00523	258839

2.3 Model Validation

In order to verify the accuracy of the battery model and the accuracy of the identification results, the battery simulation model is built in MATLAB/Simulink, and the internal parameters obtained from the offline identification are brought in, and then the accuracy can be proved by comparing the end voltages of the experiment and the simulation. This time, the current under HPPC working condition is used as input, and the comparison of simulated and experimental end voltages obtained are shown in Figures 6 and 7.

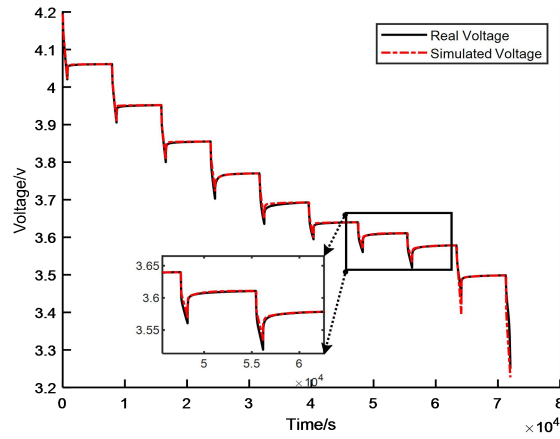


Fig. 6 Comparison curve of model end voltage

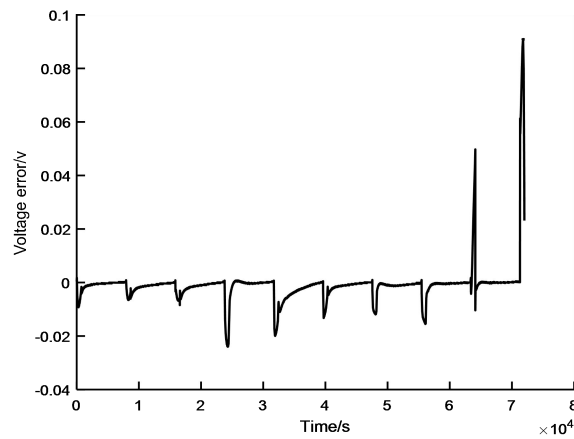


Fig. 7 Model end voltage error curve

From the above figure, it can be found that the model error only increases significantly at the end of discharge, which is caused by the intense chemical reaction inside the battery, and the terminal voltage error at the rest of the stages is within 0.04 V, which meets the battery model accuracy requirements. It proves that the constructed battery model has high accuracy and parameter identification accuracy, which lays the foundation for the next step of battery SOC estimation.

3.SVD-UKF Estimation of Battery SOC

3.1 UKF algorithm

UKF is based on the untraceable (UT) transform, which can estimate the battery condition more accurately. The basic principles of UT transform and UKF and the UKF process for estimating battery SOC are given below.

UT transform is the key step of UKF, and $2n+1$ Sigma points can be obtained by sampling according to the symmetric distribution. The formula is shown in the following equation.

$$\begin{cases} X^i = \hat{x}, i = 0 \\ X^i = \hat{x} + (\sqrt{(n + \lambda)P})_i \quad i = 1, 2, 3, \dots, n \\ X^i = \hat{x} - (\sqrt{(n + \lambda)P})_{i-n} \quad i = n + 1, n + 2, \dots, 2n \end{cases} \quad (10)$$

The corresponding weights are:

$$\begin{cases} \omega_m^0 = \lambda / (n + \lambda) \\ \omega_c^0 = \lambda / (n + \lambda) + (1 - \alpha^2 + \beta) \\ \omega_m^i = \omega_c^i = \lambda / 2(n + \lambda) \quad i = 1, 2, \dots, 2n \end{cases} \quad (11)$$

Where, n is the dimension of the state variable; λ is the dispersion factor, the selection of which determines the proximity between the sampling points and the mean value, and usually takes a positive number between 10^{-6} ~1; α is the distribution factor of the calibration front, and $\alpha=2$ is the optimal for Gaussian distribution; β is the auxiliary scale factor to satisfy the value of 0; and γ is the scale parameter, and γ is the scaling parameter, and γ is the scaling parameter, and γ is the scaling parameter, and the scaling parameter, and is the scaling parameter. Reasonable adjustment of α and β can improve the estimation accuracy of the algorithm.

Nonlinear Transfer Processing of Sigma Point Sets.

$$y^i = f(X^i) \quad (i = 0, 1, \dots, 2n) \quad (12)$$

$$\hat{y} = \sum_{i=0}^{2n} \omega_m^i y^i \quad (13)$$

$$P_y = \sum_{i=0}^{2n} \omega_c^i (y^i - \hat{y})(y^i - \hat{y})^T \quad (14)$$

UKF estimates the battery SOC process as follows:

(1) Initialize state variable means and covariances:

$$\begin{cases} \hat{X}_0 = E[\hat{X}_0] \\ P_0 = E[(X_0 - \hat{X}_0)(X_0 - \hat{X}_0)^T] \end{cases} \quad (15)$$

(2) Condition prediction:

$$\begin{cases} X_{k|k-1}^i = f(X_{k-1}^i, u_{k-1}) \\ \hat{X}_{k|k-1}^- = \sum_{i=0}^{2n} \omega_m^i x_{k|k-1}^i \end{cases} \quad (16)$$

(3) Temporal updating of state variable error covariances:

$$\begin{cases} y_{k|k-1}^i = h(X_{k|k-1}^i, u_k), i = 0, 1, \dots, 2n \\ \hat{y}_{k|k-1}^- = \sum_{i=0}^{2n} \omega_m^i y_{k|k-1}^i \end{cases} \quad (17)$$

(4) Temporal updating of error covariances:

$$\begin{cases} P_{yy,k} = \sum_{i=0}^{2n} \omega_c^i [y_{k|k-1}^i - \hat{y}_{k|k-1}^-][y_{k|k-1}^i - \hat{y}_{k|k-1}^-]^T + R_K \\ P_{Xy,k} = \sum_{i=0}^{2n} \omega_c^i [X_{k|k-1}^i - \hat{X}_{k|k-1}^-][y_{k|k-1}^i - \hat{y}_{k|k-1}^-]^T \end{cases} \quad (18)$$

(5) Calculate the Kalman gain:

$$K_k = P_{xy,k} / P_{yy,k} \quad (19)$$

(6) Update the state variables and covariance matrix of the system:

$$\begin{cases} \hat{X}_k^+ = \hat{X}_k^- + K_k (y_k - \hat{y}_{k|k-1}^-) \\ P_k^+ = P_k^- - K_k P_{yy,k} K_k^T \end{cases} \quad (20)$$

3.2 The SVD-UKF algorithm

The first step of the UKF algorithm is to perform a traceless transformation of the state variables at the previous moment, where the central step is to obtain the square root of the covariance matrix P . A common method for calculating the square root of the matrix is the Cholesky transformation, but this method is only valid when the matrix is semi-positive definite. In real working conditions, the covariance matrix P may be non-positive definite due to unknown noise and computational errors, which leads to the dispersion of the algorithm.

A singular value decomposition of the error covariance matrix is performed:

$$P = U \Lambda V^T = U \begin{bmatrix} S & 0 \\ 0 & 0 \end{bmatrix} V^T \quad (21)$$

Where P denotes the matrix to be decomposed, U and V are two orthogonal matrices, and V is a diagonal matrix which can be rewritten as:

$$\sqrt{P} = U \sqrt{\Sigma} \quad (22)$$

This can be obtained using the combination of Eq. (22) and Eq. (10):

$$\begin{cases} X^i = \hat{x}, i = 0 \\ X^i = \hat{x} + (\sqrt{(n+\lambda)} U \sqrt{\Sigma})_i, i = 1, 2, 3, \dots, n \\ X^i = \hat{x} - (\sqrt{(n+\lambda)} U \sqrt{\Sigma})_{i-n}, i = n+1, n+2, \dots, 2n \end{cases} \quad (23)$$

4. Simulation Verification and Analysis

The improved traceless Kalman filter algorithm is used to estimate the SOC of the Li-ion battery. The initial value of SOC is defined as 0.9, which is used to verify the convergence of the SVD-UKF algorithm. The estimation accuracy of UKF and SVD-UKF is compared by using the ampere-time integration method as the real estimation result, and the estimation results are shown in Fig. 8 and Fig. 9.

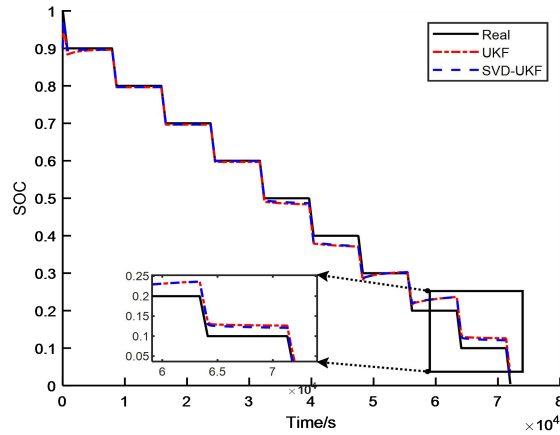


Fig. 8 SOC curve

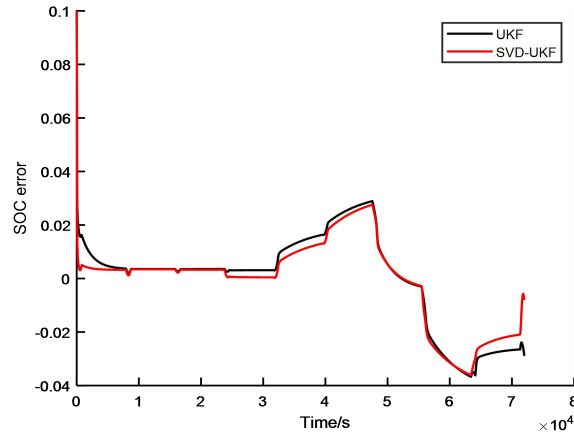


Fig. 9 SOC error curve

Table 2 Comparison of UKF and SVD-UKF errors

Algorithm	Mean error	absolute Maximum absolute error	Root square error	mean
UKF	1.3154%	3.6748%	1.7269%	
SVD-UKF	1.1234%	3.6102%	1.5603%	

As can be seen from the figure and table, the SVD-UKF algorithm has significantly better accuracy than the UKF algorithm in estimating SOC. Whether in terms of average absolute error, maximum absolute error or root mean square error, SVD-UKF performs better. The SVD-UKF algorithm converges faster during the estimation process, especially during the time period of larger error, SVD-UKF can adjust its estimation value more quickly to make it closer to the real value. Compared with the traditional UKF, the average absolute error is reduced by about 14.5%, the maximum absolute error is reduced by about 1.7%, and the root mean square error is reduced by about 9.6%.

The covariance matrix P is changed to $P = -1e-2 \cdot \text{diag}([1 \ 1 \ 1])$, at this time the covariance matrix is a non-positive definite matrix to judge the stability of the SVD-UKF algorithm, and at this time, the initial value is changed to 0.8 to judge the robustness of the SVD-UKF. The results are shown in Fig. 10.

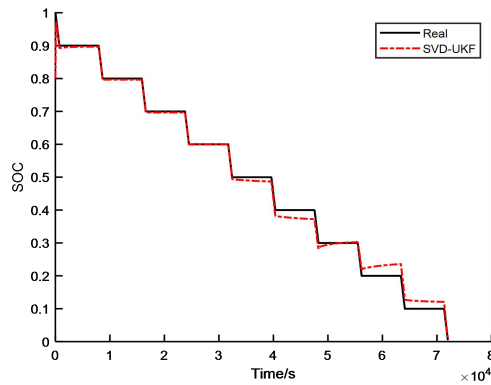


Fig. 10 SVD-UKF estimated SOC curve

From the figure, we can see that when the covariance matrix is a non-positive definite matrix and the initial value is large, the SVD-UKF algorithm can still run normally and converge to the real value quickly, which proves that the algorithm has good stability and robustness.

5. Conclusions

In this paper, the equivalent circuit model of the second-order RC equivalent circuit of the lithium battery is established, and the parameters in the model are identified using matlab and 1stopt, and the simulation model of the lithium battery is established in Matlab, and then the traditional UKF is improved for estimating the SOC of the battery, and the SOC values obtained by the SVD-UKF and the traditional UKF are compared with the actual values, which indicates that the improved algorithm can effectively estimate the SOC value.

References

- [1] Tan Zefu, Sun Rongli, Yang Rui, et al. A review of the development of battery management system [J]. Journal of Chongqing University of Technology (Natural Science), 2019, 33(9):40-45.
- [2] Genxing Liao, Yingying Zhao, Yanfeng Gao, et al. Model parameter identification and charge state estimation of lithium-ion batteries[J]. Power Supply Technology, 2021, 45(9):1136-1139.
- [3] Ko C J, Chen K C. Using tens of seconds of relaxation voltage to estimate open circuit voltage and state of health of lithium ion batteries[J]. Applied Energy, 2024, 357: 122488.
- [4] Ouyang J, Lin H, Hong Y. Whale optimization algorithm BP neural network with chaotic map** improving for SOC estimation of LMFP battery[J]. Energies, 2024, 17(17): 4300.
- [5] Monirul I M, Qiu L, Ruby R. Accurate SOC estimation of ternary lithium-ion batteries by HPPC test-based extended Kalman filter[J]. Journal of Energy Storage, 2024, 92: 112304.
- [6] Wang S, Huang P, Lian C, et al. Multi-interest adaptive unscented Kalman filter based on improved matrix decomposition methods for lithium-ion battery state of charge estimation[J]. Journal of Power Sources, 2024, 606: 234547.
- [7] Jiang Qin, Zhang Xuanxiong. Model parameter identification and charge state estimation of lithium-ion battery for electric vehicles[J]. Electronic Science and Technology, 2020, 33(2):32-36.
- [8] Wang Shifan, Luo Yang, Dong Liang, et al. Offline identification of the parameters of the second-order Thevenin lithium battery equivalent model [J]. Electronic Design Engineering, 2018, 26(9):46-49. .
- [9] Li Huan, Wang Shunli, Zou Chuanyun, et al. Research on SOC estimation based on Thevenin model and adaptive Kalman [J]. Automation Instrumentation, 2021, 42(1):46-51.